

Luttinger-Ward functional approach in the Eliashberg framework: A systematic derivation of scaling for thermodynamics near the quantum critical point

A Benlagra^{1,3}, K-S Kim² and C Pépin^{1,4}

1 Institut de Physique Théorique, CEA, IPhT, CNRS, URA 2306, F-91191 Gif-sur-Yvette, France

2 Asia Pacific Center for Theoretical Physics, Hogil Kim Memorial building 5th floor, POSTECH, Hyoja-dong, Namgu, Pohang 790-784, Korea

3 Institut für Theoretische Physik, Technische Universität Dresden, 01062 Dresden, Germany.

4 International Institute of Physics, Universidade Federal do Rio Grande do Norte, 59078-400 Natal-RN, Brazil

E-mail: adel.benlagra@mailbox.tu-dresden.de

Abstract. Scaling expressions for the free energy are derived, using the Luttinger-Ward (LW) functional approach in the Eliashberg framework, for two different models of quantum critical point (QCP). First, we consider the spin-density-wave (SDW) model for which the effective theory is the Hertz-Moriya-Millis (HMM) theory, describing the interaction between itinerant electrons and collective spin fluctuations. The dynamic of the latter are described by a dynamical exponent z depending on the nature of the transition. Second, we consider the Kondo breakdown model for QCP's, one possible scenario for heavy-fermion quantum transitions, for which the effective theory is given by a gauge theory in terms of conduction electrons, spinons for localized spins, holons for hybridization fluctuations, and gauge bosons for collective spin excitations. For both models, we construct the thermodynamic potential, in the whole phase diagram, including all kinds of self-energy corrections in a self-consistent way, at the one loop level. We show how Eliashberg framework emerges at this level and use the resulting Eliashberg equations to simplify the LW expression for free energy. It is found that collective boson excitations play a central role. The scaling expression for the singular part of the free energy near the Kondo breakdown QCP is characterized by two length scales: one is the correlation length for hybridization fluctuations, and the other is that for gauge fluctuations, analogous to the penetration depth in superconductors.

PACS numbers: 71.10.Hf, 71.30.+h, 71.10.-w, 71.10.Fd

1. Introduction

Fluctuation corrections are an essential ingredient near quantum critical points (QCPs). It may be relatively easy to incorporate quantum corrections in the weak coupling approach, the so called Hertz-Moriya-Millis (HMM) theoretical framework [1]. However, it becomes more complicated to include quantum fluctuations in the strong coupling approach such as the gauge theoretical framework sometimes proposed to describe strongly correlated electrons like doped Mott insulators [2] and some heavy-fermion QCPs [3]. For these models, it is believed that strong correlations fractionalize electrons into some exotic elementary excitations carrying fractional quantum numbers of electrons, and quantum fluctuations of such enhanced degrees of freedom appear to be complicated. It is challenging to develop a systematic approach to introduce, self-consistently, physically essential fluctuations into the thermodynamic potential near a QCP.

Effects of quantum corrections on the thermodynamic potential can be incorporated systematically using the Luttinger-Ward (LW) functional approach [4, 5, 6], where the grand potential is written in terms of dynamic quantities, such as the fully dressed Green's function $G[\Sigma]$ and the self-energy Σ , through the relation[6]

$$\Omega[\Sigma] = T \text{STr} \left[\ln \left\{ -G^{-1}[\Sigma] \right\} + \Sigma G[\Sigma] \right] + Y \left\{ G[\Sigma] \right\}, \quad (1)$$

where $\text{STr}[A] = \text{Tr}[A_B] - \text{Tr}[A_F]$ is the supertrace over Matsubara frequencies, internal quantum numbers of the bosonic (B) and fermionic (F) components of A. The quantity $Y \left\{ G[\Sigma] \right\}$ is the so-called LW functional, determined purely by the interaction potential and given by the sum of all closed-loop two-particle irreducible skeleton diagrams in the perturbation theory approach. Variation of the LW functional Y with respect to G generates the self-energy

$$\frac{\delta Y \left\{ G[\Sigma_s] \right\}}{\delta G[\Sigma_s]} = \Sigma_s \equiv G_0^{-1} - G^{-1}[\Sigma_s] \quad (2)$$

where G_0 is the non-interacting Green's function.

The thermodynamic potential is stationary with respect to changes of the self-energy, i.e. it satisfies the saddle-point condition

$$\left. \frac{\delta \Omega[\Sigma]}{\delta \Sigma} \right|_{\Sigma = \Sigma_s} = 0. \quad (3)$$

An important issue in the perturbation approach of the LW functional is to find an explicit functional dependence for Y [7]. This is generally unknown and it is not always possible to sum the skeleton expansion into a closed form for Y . The problem with strongly correlated systems is even worse because the convergence of the skeleton expansion is not guaranteed. It was demonstrated that the LW functional can be written as a closed form in the Eliashberg framework [9, 10], where the Eliashberg approximation allows to handle quantum corrections in a self-consistent way, at the one-loop level. The Eliashberg theory turns out to be justified for $z > 1$ quantum criticality, where z is the dynamical exponent, using a large- N expansion supporting the Migdal theorem

[11]. Here N is the number of fermion flavors with spin symmetry $SU(2)$. In particular, the Eliashberg theory was argued to be a minimal framework well working near a QCP [10].

In this study, we derive a LW expression of the free energy for two models of itinerant QCPs : the spin-density-wave (SDW) model and the Kondo breakdown model. This will allow us to describe thermodynamics near these QCPs starting from a microscopic model and incorporating self-consistently the effect of quantum fluctuations. It is the first time that this is done for the Kondo breakdown model.

The plan is as follows. In section 2, we present the Spin-fermion (SF) model and derive in a systematic way the LW functional and show how Eliashberg equations for self-energies are derived. The expression of the free energy is simplified using Eliashberg equations and the scaling expression of its singular part is deduced. Section 3 is devoted to the Kondo Breakdown (KB) model. A particular care is taken to describe the Higgs part of the phase diagram. The effect of condensation is incorporated into a zero-order theory before considering a cumulant expansion in the fluctuations interaction. For this gauge theory, there are additional collective excitations, which results in the presence of two length scales in the scaling expression of the free energy. These two scales are related through the Anderson-Higgs mechanism. Section 4 summarizes and discusses our main results. In particular, theoretical structure differences between the HMM theory and the gauge theory of the Kondo breakdown QCP are emphasized. Technical details are presented in the appendices.

2. Review of the Luttinger-Ward functional approach in the Eliashberg framework of the spin-fermion model

The standard model of quantum criticality in a metallic system is the HMM theory. In this model, a dynamical exponent z , relating the variation of the energy with the momentum $\omega \sim q^z$, characterizes the dynamics of collective excitations near the QCP. In particular, $z = 3$ describes the ferromagnetic QCP while $z = 2$ describes the antiferromagnetic one. It is valuable to review the construction of the LW functional in the HMM theoretical framework, discussed in the past[9], although several heavy fermion compounds have been shown not to follow the $z = 2$ HMM theory [16, 17, 18, 19, 20].

2.1. Spin-fermion model

We start from the so called spin-fermion model (SF) [10, 21, 22] for the SDW transition

$$\begin{aligned} \mathcal{S}_{SF} = & T \sum_k \psi_{\sigma k}^\dagger [-G_0^{-1}(k)] \psi_{\sigma k} + \frac{1}{2} T \sum_q \chi_0^{-1}(q) \vec{S}_q \cdot \vec{S}_{-q} \\ & + g T^2 \sum_k \sum_q \psi_{\sigma k+q}^\dagger \vec{\tau}_{\sigma\sigma'} \psi_{\sigma' k} \cdot \vec{S}_{-q} + \mathcal{O}[\{\vec{S}\}^n; n \geq 3], \end{aligned} \quad (4)$$

where we used the "relativistic" notation for energy-momentum $k \equiv (\mathbf{k}, i\omega)$, $q \equiv (\mathbf{q}, i\Omega)$ and the sum expression is defined as

$$\sum_k \dots \equiv \sum_{i\omega} \int_{|\mathbf{k}-\mathbf{k}_F|<\Lambda} \frac{d^d k}{(2\pi)^d} \dots, \quad \sum_q \dots \equiv \sum_{i\Omega} \int_{|\mathbf{q}-\mathbf{Q}|<\Lambda} \frac{d^d q}{(2\pi)^d} \dots$$

In (4), $\psi_{\sigma k}$ is the fermionic annihilation field for an electron with energy-momentum vector k and spin σ , \vec{S}_q is a bosonic field describing spin-fluctuations near a momentum \mathbf{Q} and g is the coupling constant measuring the strength of the interaction between fermionic and bosonic excitations. The last term in (4) stands for higher order terms in S . These are shown to be irrelevant for $d > 2$ and marginal for $d = 2$ and can therefore be neglected [22].

In the absence of the interaction, fermionic and bosonic excitations are described by the bare electron Green's function $G_0(k)$ and the bare spin susceptibility $\chi_0(q)$ respectively

$$G_0(k) = \frac{z_0}{i\omega - v_F|\mathbf{k} - \mathbf{k}_F|}, \quad \chi_0(q) = \frac{\chi_0}{\xi_0^{-2} + |\mathbf{q} - \mathbf{Q}|^2 + \Omega^2/v_s^2}. \quad (5)$$

z_0 is the quasiparticle renormalization factor given by the Fermi liquid theory, and the electron dispersion is linearized with a Fermi velocity v_F and Fermi momentum \mathbf{k}_F . The electron's chemical potential can incorporate effects of the condensed part of the bosonic field. The bare spin susceptibility is the usual Ornstein-Zernicke form where ξ_0 is the bare correlation length of spins and $\chi_0\xi_0^2$ is the static susceptibility. v_s is the bare spin velocity.

The spin-fermion model Eq.(4) is an effective low-energy model that can be derived from the Hubbard-like model in the weak coupling approximation [10, 21, 22]; high-energy fermions, with energy above Λ , are integrated out to generate collective bosonic modes that mediate the interaction between fermions at energies smaller than Λ . Dynamics of the low-energy fermions and the collective spin excitations are then described by Eq. (5).

2.2. Eliashberg theory

The Eliashberg framework allows the evaluation of the self-energies Σ and Π , for electrons and spin fluctuations respectively, self-consistently assuming we can neglect the momentum dependence of the Σ and vertex corrections. An extensive review of this technique is given in [10]. We recall here the spirit of this technique and main results.

The Eliashberg procedure relies on three steps:

- neglect both the vertex corrections and the momentum dependence of the fermionic self-energy :

$$\Sigma(\mathbf{k}, i\omega_n) = \Sigma(i\omega_n), \quad \Delta g = 0$$

- Use Dysons' equations

$$\begin{aligned} G^{-1}(\mathbf{k}, i\omega_n) &= G_0^{-1}(\mathbf{k}, i\omega_n) - \Sigma(i\omega_n), \\ \chi^{-1}(\mathbf{q}, i\Omega_n) &= \chi_0^{-1}(\mathbf{q}, i\Omega_n) - \Pi(\mathbf{q}, i\Omega_n), \end{aligned} \quad (6)$$

to evaluate self-consistently the self-energies represented diagrammatically in Fig.-1(a) and (c), where the propagators are fully dressed according to (6).

- Check *a posteriori* that the neglected momentum dependence of the fermionic self-energy and vertex corrections are indeed small.

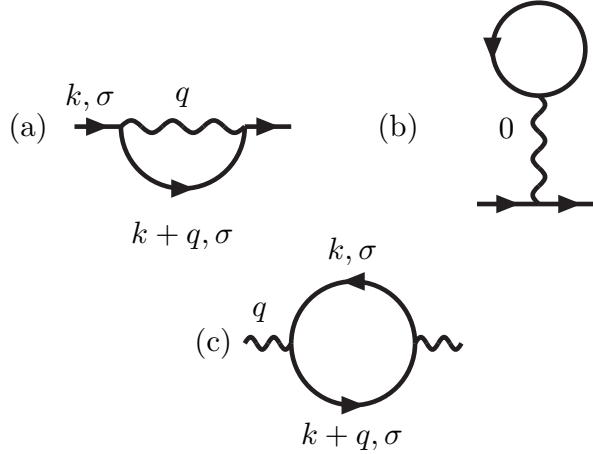


Figure 1. (a) and (b) are the first order contribution to the fermionic self-energy and (c) is the polarization bubble, where $\sigma \in [1, N]$ is the spin index. The propagators of the fermion (straight line) and the spin fluctuations boson (wavy line) are fully dressed. (b) is a static and uniform part in the self-energy and can thus be considered as a renormalization of the electron chemical potential.

The bosonic self-energy is found to be

$$\Pi(\mathbf{q}, i\Omega_n) = \gamma \frac{|\Omega_n|}{q^{z-2}}, \quad (7)$$

where $\gamma = g^2 \chi_0 k_F / (\pi v_F^2)$ and z is the dynamical exponent. This result is customary for problems where fermions interact with their own collective modes. The latter are damped whenever they lie inside the particle-hole continuum of the Fermi liquid[1]. Such a Landau-damped term is larger than the regular $\mathcal{O}(\Omega^2)$ term in the bare spin susceptibility Eq.(5) and fully determines the collective spin dynamics. This causes feedback effects on the self-energy correction of electrons, giving rise to non-Fermi liquid physics near the QCP[10].

The model (4) can be extended by introducing $N \neq 1$ identical fermionic species with spin symmetry $SU(2)$ ‡. A channel index $\nu \in [1, N]$ is then added to the fermionic operators ψ in (4) and $g \rightarrow g/\sqrt{N}$ to ensure a well-defined large N limit.

‡ A problem in using the $SU(N)$ representation arises for the definition of the spin operator which is only possible in the $Sp(N)$ representation. This is a crucial aspect in particular when considering the spin fluctuations as critical modes. Then either we use the $Sp(N)$ representation or N copies of $SU(2)$ fermions.

It has been shown that the Eliashberg approximation becomes exact in the limit $N \rightarrow \infty$ [9, 21]. Indeed, it is shown that both vertex corrections and the momentum-dependent corrections to the fermionic self-energy turn out to scale as $1/N$ and vanish in the limit $N \rightarrow \infty$. This limit shares some similarity with the Migdal limit for the electron-phonon problem : at large N , the damping introduced in (7) scales as N and the collective excitations become slow. Then, the smallness in $1/N$ compares to the smallness in m/M where m is the electron's mass and M is the ion's mass.

In the following, we will show how the Eliashberg framework emerges from the LW approach to the Spin-Fermion model.

2.3. Luttinger-Ward functional for the spin-fermion model

As said in the introduction, the LW functional is, diagrammatically, the sum of all closed-loop two-particle irreducible skeleton diagrams[4]. These can be ordered in a $1/N$ expansion as in Fig.-2

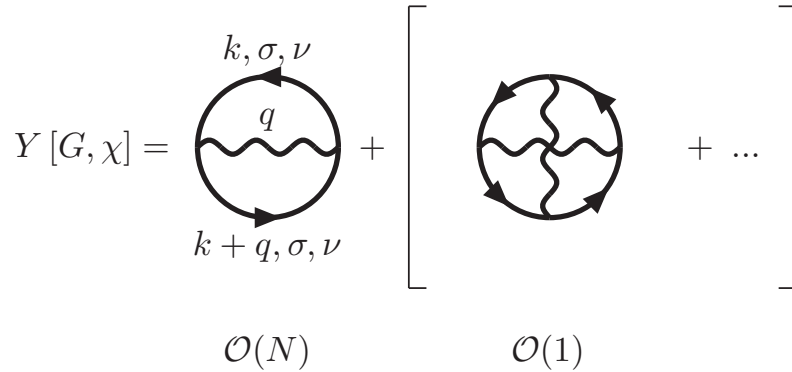


Figure 2. Leading skeleton diagrams participating to the LW functional Y for the Spin-Fermion model with dependence on $1/N$. Fermion (straight line) and boson (wavy line) propagators are fully dressed, $\sigma \in [1, N]$ is the spin index and $\nu \in [1, N]$ is the channel index. The first diagram contains one fermionic loop carrying spin and channel quantum numbers and one pair of vertices, each of order $\mathcal{O}(1/\sqrt{N})$, so that it is of order $\mathcal{O}(N^2/N) = \mathcal{O}(N)$. The second diagram involves one fermionic loop and two pairs of vertices so that it is of order $\mathcal{O}(N^2/N^2) = \mathcal{O}(1)$. Bracketed terms are dropped in the large N limit.

Considering the general expression of the LW expression [Eq.(1)], and taking into account only the leading $\mathcal{O}(N)$ contribution to Y , shown in Fig.-2 and derived in Appendix A, one can write down the free energy in terms of electron and spin-fluctuation Green's functions and self-energies

$$\begin{aligned}
 F_{LW}[\Sigma, \Pi] = & -NT \sum_k \left[\ln \left\{ -G^{-1}(k) \right\} + \Sigma(k)G(k) \right] + T \sum_q \left[\ln \left\{ \chi^{-1}(q) \right\} + \Pi(q)\chi(q) \right] \\
 & + 3Ng^2T^2 \sum_{k,q} G(k)\chi(q)G(k+q), \tag{8}
 \end{aligned}$$

where $G(k)$ and $\Sigma(k)$ are the fully renormalized electron Green's function and self-energy, while $\chi(q)$ and $\Pi(q)$ are the fully renormalized spin-fluctuation Green's function and self-energy. The last term in (8) corresponds to the leading skeleton diagram of order $\mathcal{O}(N)$ shown in Fig.-2.

2.4. Eliashberg equations

One of the important aspects of the LW functional approach is that we can recover the self-consistent Eliashberg equations for self-energies. Indeed, if we restrict ourselves to the leading $\mathcal{O}(N)$ term in Y and use the stationarity of the free energy (8) with respect to self-energies (3), we get the following equations

$$\begin{aligned} \frac{\delta G}{\delta \Sigma} \left(-\Sigma(k) + 3g^2 T \sum_q G(k+q)\chi(q) \right) &= 0, \\ \frac{\delta \chi}{\delta \Pi} \left(\Pi(q) + 3Ng^2 T \sum_k G(k+q)G(k) \right) &= 0, \end{aligned}$$

from which we deduce immediately the expressions of the electronic self-energy and the collective spin polarization

$$\begin{aligned} \Sigma(k) &= 3g^2 T \sum_q G(k+q)\chi(q), \\ \Pi(q) &= -3Ng^2 T \sum_k G(k+q)G(k). \end{aligned} \quad (9)$$

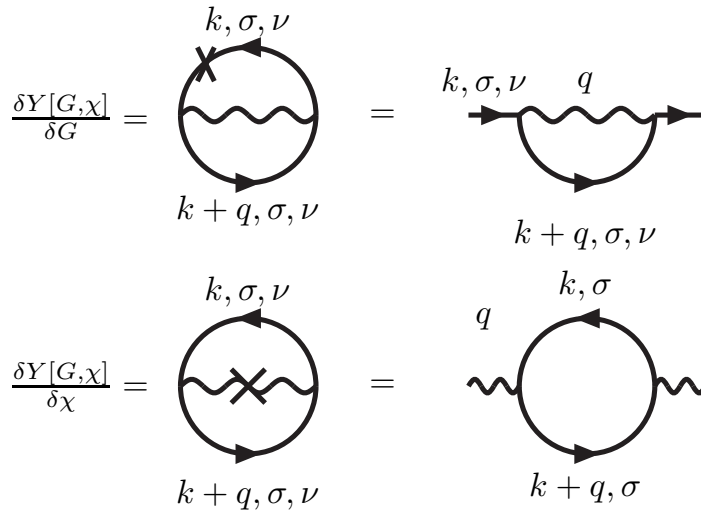


Figure 3. Illustrating functional derivative of the LW functional with respect to Green's functions. The cross indicates the line that is cut by functional differentiation.

These expressions can be also obtained by differentiating the leading order $\mathcal{O}(N)$ contribution to the LW functional Y with respect to G and χ respectively, according to equation (2). Diagrammatically, this is equivalent to cutting one of the internal lines of

the corresponding diagram, as shown in Fig.-3.

Equations (9), with Dyson's equations, are nothing but the self-consistent Eliashberg equations for self-energies (see Fig.1).

Considering further terms in the LW functional Y amounts to studying deviations from the Eliashberg theory, in particular introducing vertex corrections as shown in Fig.-4, in the $1/N$ expansion.

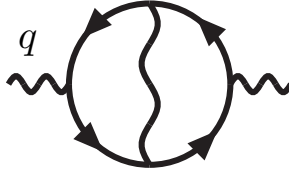


Figure 4. Spin-fluctuations self-energy generated from the contribution to the LW functional of order $\mathcal{O}(1)$, shown in Fig.2, by cutting one internal bosonic line. This can be obtained from The Eliashberg form of the spin-fluctuations polarization shown in Fig.-1(c) by inserting a bosonic propagator to the vertex.

2.5. Simplification of the Luttinger-Ward expression

One can simplify further the full expression Eq.(8) of the free energy [9]. Indeed, from equations (9), one can notice that

$$\begin{aligned} Y \{G, \chi\} &\equiv 3Ng^2T^2 \sum_{k,q} G(k)\chi(q)G(k+q) \\ &= NT \sum_k \Sigma(k)G(k) \end{aligned} \quad (10)$$

$$= -T \sum_q \Pi(q)\chi(q). \quad (11)$$

Thus, if we insert Eq. (11) into Eq.(8), the latter reduces to

$$F_{eff} = -NT \sum_k \left[\ln\{-G^{-1}(k)\} + \Sigma(k)G(k) \right] + T \sum_q \ln\{\chi^{-1}(q)\}, \quad (12)$$

while if we insert Eq. (10) we get the following expression for Eq.(8)

$$F_{eff} = -NT \sum_k \ln\{-G^{-1}(k)\} + T \sum_q \left[\ln\{\chi^{-1}(q)\} + \Pi(q)\chi(q) \right]. \quad (13)$$

Considering equation (12), we can show (See Appendix B.1) that the fermionic part reduces to a Fermi liquid form $F_{FL} \equiv -\frac{\pi N \rho_F}{6} T^2$ so that the final expression of the free energy for thermodynamics in the Eliashberg framework writes

$$F_{eff} = F_{FL} + T \sum_q \ln\{\chi^{-1}(q)\}. \quad (14)$$

2.6. Thermodynamics

Performing the energy and momentum integrals in the Eliashberg equations Eq. (9), one finds [21, 22]

$$\Pi(\mathbf{q}, i\Omega) = \gamma \frac{|\Omega|}{q^{z-2}}, \quad (15)$$

where $\gamma = Ng^2\chi_0k_F/(\pi v_F^2)$. Considering only the linear-frequency Landau term in the spin susceptibility, this writes

$$\chi^{-1}(\mathbf{q}, i\Omega) = \chi_0^{-1} \left(\xi^{-2} + |\mathbf{q} - \mathbf{Q}|^2 + \frac{|\Omega|}{q^{z-2}} \right). \quad (16)$$

In particular, we have $z = 2$ for an antiferromagnetic QCP and $z = 3$ for a ferromagnetic one.

Using this expression, the singular part of the free energy (14) writes

$$\begin{aligned} f_s(\xi^{-2}, T) &= T \sum_{i\Omega, q} \ln \left\{ \xi^{-2} + |\tilde{q}|^2 + \gamma \frac{|\Omega|}{q^{z-2}} \right\} \\ &= -\frac{1}{\pi} \int_0^\infty d\nu \coth\left(\frac{\nu}{2T}\right) \int \frac{d^d \tilde{q}}{(2\pi)^d} \tan^{-1} \left(\frac{\gamma\nu/\tilde{q}^{z-2}}{\xi^{-2} + \tilde{q}^2} \right), \end{aligned} \quad (17)$$

where $\tilde{\mathbf{q}} = \mathbf{q} - \mathbf{Q}$ is the shifted momentum near the wave vector \mathbf{Q} . Performing the frequency and momentum integrals in this equation, one finds the analytic expression of (17). Details of this evaluation for $d = 3, z = 2$ are given in appendix Appendix C.

We would like to emphasize that the resulting effective free energy satisfies the following scaling relation

$$f_s(r, T) = b^{-(d+z)} f_r(rb^{1/\nu}, Tb^z), \quad (18)$$

where $f_r(x, y)$ is an analytic regular function. $r \sim \xi^{-2}$ measures the distance to the QCP[§], ν is the correlation-length exponent, z is the dynamical exponent and d is the space dimension. Inserting $b = \xi^{2\nu}$ into the above scaling expression, we find

$$f_s(\xi^{-2}, T) = \xi^{-2\nu(d+z)} f_r(1, T\xi^{2\nu z}). \quad (19)$$

Now, one can understand thermodynamics near the HMM theory QCP based on this scaling free energy, derived from the effective field theory in the Eliashberg framework.

As is already known, the naive scaling (18) may be spoiled by the presence of at least one dangerously irrelevant variable [1] leading to a generalized scaling form

$$f(\xi^{-2}, T, u) = b^{-(d+z)} f(\xi^{-2}b^{1/\nu}, Tb^z, ub^{d+z-4}), \quad (20)$$

where u is the constant coefficient of an additional ϕ^4 term in the theory.

[§] Within the Eliashberg approximation, the correlation length's critical exponent value $\nu = 1/2$, coming from the Ornstein-Zernicke form for the static boson propagator in Eqs. (5, 16) and valid at high energy, has no quantum corrections. This coincides with its mean-field value in the Hertz theory above the upper critical dimension, i.e. when $d + z > 4$.

In practice, for thermodynamics quantities, the results obtained from the naive scaling hold up to logarithmic corrections where the argument of the logarithm is a power of T . We comment in Appendix E on how the effect of such variables can be handled within our method and show that we can obtain the same generalized expression (20). The purpose in this section is only to show how one can get an analytic expression for free energy including quantum corrections in a self-consistent way.

3. Luttinger-Ward functional in the Eliashberg framework of the Kondo breakdown scenario

The HMM theoretical framework has been regarded as the standard model for quantum criticality in metals for a long time, although several heavy fermion compounds have been shown not to follow its predictions [16, 17, 18, 19, 20]. An interesting alternative theory suggests that heavy fermion quantum transitions are selective Mott transitions of the f nearly localized fermions [13, 14, 15, 24] at which the Kondo effect breaks down. This scenario is supported by the presence of localized magnetic moments at the transition towards magnetism [17] and Fermi surface reconstruction at the QCP [18, 19].

This problem has been tackled using the U(1) slave-boson representation of the Anderson lattice model [14, 15], with the introduction of a small dispersion for the f -electrons. A remarkable aspect of the theory is that the resulting QCP, at which an effective hybridization vanishes, is multi-scale. Indeed, because we have two kind of fermions in the model, i.e the conduction c -fermions and the f -spinons, there exist a Fermi surface mismatch $q^* = |k_F^f - k_F^c|$ between Fermi momentum k_F^f for spinons and k_F^c for conduction electrons since fillings of spinons and electrons differ from each other. This mismatch gives rise to an energy gap E^* for spinon-electron fluctuations that controls the dynamics of hybridization fluctuations. Although it depends on the value of q^* , this energy scale is shown to vary from $\mathcal{O}(10^0) mK$ to $\mathcal{O}(10^2) mK$. When $E < E^*$, holon fluctuations are undamped, thus described by $z = 2$ dynamical exponent. On the other hand, when $E > E^*$, holon fluctuations are dissipative since spinon-electron excitations are Landau damped, thus described by $z = 3$ critical theory. Based on the $z = 3$ quantum criticality, recent studies have found quasi-linear electrical transport and logarithmically divergent specific heat coefficient in $d = 3$ [15, 14, 25], and a divergent Grüneisen ratio with an anomalous exponent 0.7 [12], consistent with experiments [16, 20].

3.1. U(1) slave-boson representation of the Anderson lattice model

We start from the Anderson lattice model in the large- U limit

$$\begin{aligned} \mathcal{L} = & \sum_i c_{i\sigma}^\dagger ((\partial_\tau - \mu)\delta_{ij} - t_{ij}) c_{j\sigma} + \sum_i d_{i\sigma}^\dagger (\partial_\tau + \epsilon_f) d_{i\sigma} \\ & + V \sum_i (d_{i\sigma}^\dagger c_{i\sigma} + H.c.) + J \sum_{\langle ij \rangle} \vec{S}_i \cdot \vec{S}_j, \end{aligned} \quad (21)$$

where $c_{i\sigma}$ and $d_{i\sigma}$ are conduction electron with a chemical potential μ and localized electron with an energy level ϵ_f , respectively, t_{ij} the hopping term of the conduction electron and V the hybridization between c- and d-electrons. The last spin-exchange term is generated by a perturbative expansion to second order in t/U and is in competition with the hybridization term.

In the $U \rightarrow \infty$ limit of (21), the strong correlations between the d-electrons show as a constraint of no double occupancy for the d-electron. This can be handled using the U(1) slave-boson representation

$$d_{i\sigma} = b_i^\dagger f_{i\sigma}, \quad (22)$$

where b_i and $f_{i\sigma}$ are holon and spinon, associated with hybridization and spin fluctuations, respectively, obeying the local constraint

$$b_i^\dagger b_i + \sum_{\sigma} f_{i\sigma}^\dagger f_{i\sigma} = SN, \quad (23)$$

where $S = 1/2$ is the value of spin and N is the number of fermion flavors with $\sigma = 1, \dots, N$.

One can then rewrite Eq. (21) into

$$\begin{aligned} \mathcal{L} = & \sum_{\langle ij \rangle} c_{i\sigma}^\dagger ((\partial_\tau - \mu)\delta_{ij} - t_{ij}) c_{j\sigma} + \sum_i f_{i\sigma}^\dagger (\partial_\tau + \epsilon_f) f_{i\sigma} + b_i^\dagger \partial_\tau b_i \\ & + V \sum_i (b_i f_{i\sigma}^\dagger c_{i\sigma} + H.c.) + J \sum_{\langle ij \rangle} (f_{i\sigma}^\dagger \chi_{ij} f_{j\sigma} + H.c.) \\ & + NJ \sum_{\langle ij \rangle} |\chi_{ij}|^2 + i \sum_i \lambda_i (b_i^\dagger b_i + f_{i\sigma}^\dagger f_{i\sigma} - SN) \end{aligned} \quad (24)$$

The spin-exchange term for the localized orbital has been decomposed, using a field χ_{ij} , resulting in exchange hopping processes for the spinons. The local constraint (23) is taken into account by the introduction of a Lagrange multiplier λ_i .

Performing the saddle-point approximation of $b_i \rightarrow b$, $\chi_{ij} \rightarrow \chi$, and $i\lambda_i \rightarrow \lambda$, one finds an orbital selective Mott transition as breakdown of Kondo effect at $J \approx T_K$, where a spin-liquid Mott insulator ($b = 0$) arises in $J > T_K$ while a heavy-fermion Fermi liquid ($b \neq 0$) results in $T_K > J$ [13, 14, 15]. Here, $T_K = D \exp\left(\frac{\epsilon_f}{N\rho_c V^2}\right)$ is the Kondo temperature, where $\rho_c \approx (2D)^{-1}$ is the density of states for conduction electrons with the half bandwidth D .

Beyond the mean-field approximation, gauge fluctuations corresponding to phase fluctuations of the hopping parameter $\chi_{ij} = \chi e^{ia_{ij}}$ should be introduced to express collective spin fluctuations. It is more convenient to represent the above effective Lagrangian as follows, performing the continuum approximation ||,

$$\mathcal{L}_{ALM} = \sum_{\sigma} \int d\mathbf{r} \quad c_{\sigma}^* (\partial_{\tau} - \mu_c) c_{\sigma} + \frac{1}{2m_c} |\partial_i c_{\sigma}|^2 + f_{\sigma}^* (\partial_{\tau} - \mu_f - ia_0) f_{\sigma}$$

|| The fermionic and bosonic fields here are all time and position dependent. A full discussion of this Lagrangian can be found in [15].

$$\begin{aligned}
& + \frac{1}{2m_f} |(\partial_i - ia_i)f_\sigma|^2 + b^*(\partial_\tau - \mu_b - ia_0)b + \frac{1}{2m_b} |(\partial_i - ia_i)b|^2 + \frac{u_b}{2} |b|^4 \\
& + V(b^*c_\sigma^*f_\sigma + H.c.) + \frac{1}{4g^2} F_{\mu\nu}F_{\mu\nu} + SN(\mu_b + ia_0),
\end{aligned} \tag{25}$$

where a_0 is the scalar gauge field, a_i is the i component of the vectorial gauge field \vec{a} , g is an effective coupling constant between matter and gauge fields, $F_{\mu\nu} \equiv \partial_\mu a_\nu - \partial_\nu a_\mu$ is the fictitious electromagnetic tensor associated with the four-potential (a_0, \vec{a}) . Furthermore, several quantities, such as fermion band masses and chemical potentials, are redefined as follows

$$\begin{aligned}
\lambda & \rightarrow -\mu_b, \quad (2m_c)^{-1} = t, \quad (2m_f)^{-1} = J\chi, \\
\mu_c & = \mu + 2dt, \quad -\mu_f = \epsilon_f + \lambda - 2Jd\chi.
\end{aligned} \tag{26}$$

In here, fermion bare bands ϵ_k^c and ϵ_k^f for conduction electrons and spinons, respectively, are treated in the continuum approximation as follows

$$\begin{aligned}
\epsilon_k^c & = -2t(\cos k_x + \cos k_y + \cos k_z) \approx -2dt + t(k_x^2 + k_y^2 + k_z^2), \\
\epsilon_k^f & = -2J\chi(\cos k_x + \cos k_y + \cos k_z) \approx -2Jd\chi + J\chi(k_x^2 + k_y^2 + k_z^2).
\end{aligned} \tag{27}$$

The band dispersion for hybridization can arise from high energy fluctuations of conduction electrons and spinons. Actually, the band mass of holons is given by $m_b^{-1} \approx NV^2\rho_c/2$, where ρ_c is the density of states for conduction electrons [14, 15]. Local self-interactions denoted by u_b can be introduced via non-universal short-distance-scale physics. One physical process for such interactions is four-point electron-spinon polarization (see Fig.- 5), giving rise to $u_b = u_0 \frac{V^4}{D^3}$ with $u_0 \approx \mathcal{O}(1)$. Because such a local interaction term results from non-universal physics, one may consider that this term is introduced phenomenologically.

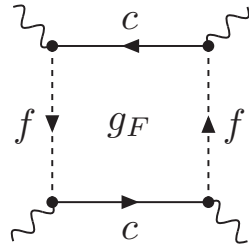


Figure 5. Four-point electron-spinon polarization for the holons.

Maxwell dynamics for gauge fluctuations appears from high energy fluctuations of spinons and holons.

We would like to develop the LW functional approach, including the Higgs or heavy-fermion phase. In this respect we write the holon field with its condensation part and fluctuation contribution separately,

$$b \rightarrow \mathcal{B} + b. \tag{28}$$

Then, the effective continuum Lagrangian is written as follows

$$\begin{aligned}
\mathcal{L}_{ALM} = & \sum_{\sigma} \int d\mathbf{r} \ c_{\sigma}^* (\partial_{\tau} + \frac{1}{2m_c} \partial_i^2 - \mu_c) c_{\sigma} + f_{\sigma}^* (\partial_{\tau} - \mu_f - ia_0) f_{\sigma} \\
& + \frac{1}{2m_f} |(\partial_i - ia_i) f_{\sigma}|^2 + b^* [\partial_{\tau} - (\mu_b - 2u_b \mathcal{B}^2) - ia_0] b + \frac{1}{2m_b} |(\partial_i - ia_i) b|^2 \\
& + \frac{u_b}{2} |b|^4 + V(b^* c_{\sigma}^* f_{\sigma} + H.c.) + V\mathcal{B}(c_{\sigma}^* f_{\sigma} + H.c.) \\
& + \frac{1}{4g^2} f_{\mu\nu} f_{\mu\nu} + \frac{\mathcal{B}^2}{2m_b} a_i^2 + \frac{u_b}{2} \mathcal{B}^4 + (SN - \mathcal{B}^2)(\mu_b + ia_0).
\end{aligned} \tag{29}$$

We see that the chemical potential for holon excitations is modified from μ_b to $\mu_b - 2u_b \mathcal{B}^2$. An important point is that gauge fluctuations become gapped when $\mathcal{B} \neq 0$, which is due to the Anderson-Higgs mechanism.

3.2. Luttinger-Ward functional in the Kondo breakdown scenario

In the following, we demonstrate how thermodynamics can be extracted from the complicated effective field theory described by (29), where two kinds of fermion excitations and two kinds of boson fluctuations are coupled with each other. The point is how to introduce all self-energy corrections self-consistently. As discussed before, we construct the LW functional in the Eliashberg framework, allowing us to take all kinds of self-energy corrections self-consistently at least in the one-loop level.

For simplicity, we start by ignoring gauge fluctuations corrections, considering only holon fluctuations. Gauge fluctuations are after that manipulated in the same way once their coupling with holons and spinons is known.

3.2.1. Constructing a zero-order theory A subtle issue in deriving a LW expression for free energy is how to handle a non-vanishing condensation $\mathcal{B} \neq 0$ to describe the Higgs phase. A first step towards this derivation is to construct a "zero-order" theory taking into account, in a proper way, the effect of the condensation part \mathcal{B} .

Going to Fourier space, we can cast the action corresponding to the Lagrangian (29) into a mean-field part and holon fluctuations part \mathfrak{N} :

$$\begin{aligned}
\mathcal{S}_{MF} = & -T \sum_k \left[c_{\sigma k}^{\dagger} g_c^{-1}(k) c_{\sigma k} + f_{\sigma k}^{\dagger} g_f^{-1}(k, i\omega) f_{\sigma k} \right] \\
& + V\mathcal{B}T \sum_k \left(f_{\sigma k}^{\dagger} c_{\sigma k} + H.c. \right) + (SN - \mathcal{B}^2) \mu_b + u_b \frac{\mathcal{B}^4}{2} \\
\mathcal{S}_{fluc} = & -T \sum_{q \neq 0} b_q^{\dagger} d_b^{-1}(q) b_q + VT^2 \sum_{k, \sigma} \sum_{q \neq 0} \left(b_k f_{\sigma k+q}^{\dagger} c_{\sigma k} + H.c. \right),
\end{aligned} \tag{30}$$

\mathfrak{N} The contribution of the local interaction with strength u_b to the LW functional is sub-leading with respect to the diagram of order $\mathcal{O}(N)$ used to derive the Eliashberg equations below. The corresponding term is thus dropped from \mathcal{S}_{fluc} . Its inclusion may result in a generalized scaling form for the free energy as shown in Appendix E.

where

$$\begin{aligned} g_c^{-1}(k) &= i\omega + \mu_c - \frac{\mathbf{k}^2}{2m_c}, \\ g_f^{-1}(k) &= i\omega + \mu_f - \frac{\mathbf{k}^2}{2m_f}, \\ d_b^{-1}(q) &= i\Omega + \mu_b - 2u_b\mathcal{B}^2 - \frac{\mathbf{q}^2}{2m_b}, \end{aligned} \quad (31)$$

The interaction term gives rise to two kind of vertices, shown in the following figures

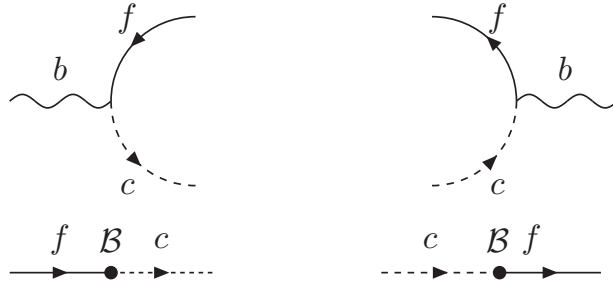


Figure 6. Vertices due to the interaction between fermions and holons. Here, a line stands for the spinon propagator, the dashed line for the electron propagator and the wavy line for the holon propagator.

Whereas it is justified to follow the same strategy as for the HMM framework (See Sec.2.3), i.e. use the cumulant expansion to the second order, for the fluctuations part of the interaction term, it is not the case for the condensation part. However, the latter can be considered as a renormalization of the propagators g_c and g_f and is thus included in a new zero-order theory whose bare action is \mathcal{S}_{MF} .

Indeed, we can write

$$\mathcal{S}_{MF} = -T \sum_{\mathbf{k}} (c_{\sigma\mathbf{k}}^\dagger \ f_{\sigma\mathbf{k}}^\dagger) G_0^{-1} \begin{pmatrix} c_{\sigma\mathbf{k}} \\ f_{\sigma\mathbf{k}} \end{pmatrix} + (SN - \mathcal{B}^2)\mu_b + u_b \frac{\mathcal{B}^4}{2}, \quad (32)$$

where

$$G_0^{-1} = \begin{pmatrix} g_c^{-1} & -V\mathcal{B} \\ -V\mathcal{B} & g_f^{-1} \end{pmatrix}.$$

This gives the renormalized matrix Green's function for the fermions

$$G_0 = \begin{pmatrix} G_{cc}^0 & G_{cf}^0 \\ G_{fc}^0 & G_{ff}^0 \end{pmatrix},$$

where

$$\begin{aligned} G_{ff}^0 &= \frac{g_c^{-1}}{g_c^{-1}g_f^{-1} - (V\mathcal{B})^2}, & G_{cc}^0 &= \frac{g_f^{-1}}{g_c^{-1}g_f^{-1} - (V\mathcal{B})^2} \\ G_{fc}^0 &= G_{cf}^0 = \frac{V\mathcal{B}}{g_c^{-1}g_f^{-1} - (V\mathcal{B})^2} \end{aligned} \quad (33)$$

The condensation renormalizes thus the propagators for the $f - f$, $c - c$ and $f - c$ channels. In fact, this equals summing the infinite series of the cumulant expansion due the condensation part of the interaction term (see Fig.-7).

$$\begin{aligned}
 G_{ff} &\equiv \text{---} \xrightarrow{f} \text{---} + \text{---} \xrightarrow{f} \bullet \text{---} \xrightarrow{c} \bullet \text{---} \xrightarrow{f} \text{---} + \text{---} \xrightarrow{f} \bullet \text{---} \xrightarrow{c} \bullet \text{---} \xrightarrow{f} \bullet \text{---} \xrightarrow{c} \bullet \text{---} \xrightarrow{f} \text{---} + \dots \\
 G_{cc} &\equiv \text{---} \xrightarrow{c} \text{---} + \text{---} \xrightarrow{c} \bullet \text{---} \xrightarrow{f} \bullet \text{---} \xrightarrow{c} \text{---} + \text{---} \xrightarrow{c} \bullet \text{---} \xrightarrow{f} \bullet \text{---} \xrightarrow{c} \bullet \text{---} \xrightarrow{f} \bullet \text{---} \xrightarrow{c} \text{---} + \dots
 \end{aligned}$$

Figure 7. Propagators of the zero-order theory, where the effect of the condensation \mathcal{B} is totally taken into account.

3.2.2. Derivation of the Luttinger-Ward functional Once we have properly handled the condensation part of the interaction, we can follow the strategy of Sec. 2.3.

The interaction term due to hybridization fluctuations writes

$$\mathcal{S}_b = \frac{V}{\sqrt{N}} T^2 \sum_{k,\sigma,\nu} \sum_{q \neq 0} \left(b_q f_{\sigma\nu k+q}^\dagger c_{\sigma\nu k} + H.c. \right), \quad (34)$$

where we have extended the model to N identical species of fermions by adding a channel index $\nu \in [1, N]$ to the fermionic operators and the $1/\sqrt{N}$ factor ensures a well-defined large- N limit.

Considering only the leading $\mathcal{O}(N)$ contribution to the LW functional shown in Fig.-8, and according to the general formula Eq.(1), we get the following expression for the free energy

$$F_{LW}^{eff} = F_F + F_b + Y_b + \left(SN - \mathcal{B}^2 \right) \mu_b + u_b \frac{\mathcal{B}^4}{2}, \quad (35)$$

with

$$\begin{aligned}
 F_F &= -T \text{Tr} \left[\ln \left(-G_0^{-1} + \Sigma \right) + \Sigma G \right] \\
 F_b &= T \text{Tr} \left[\ln \left(-d_b^{-1} + \Pi_b \right) + \Pi_b D_b \right] \\
 Y_b &= -2NV^2 \sum_k \sum_{q \neq 0} D_b(q) G_{cc}(k) G_{ff}(k+q)
 \end{aligned} \quad (36)$$

In (36), $\Sigma = \begin{pmatrix} \Sigma_{cc} & \Sigma_{cf} \\ \Sigma_{fc} & \Sigma_{ff} \end{pmatrix}$ and $G = \begin{pmatrix} G_{cc} & G_{cf} \\ G_{fc} & G_{ff} \end{pmatrix}$ are the self-energy and full Green's matrices, respectively, of the fermions. They are related by the Dyson's equation

$$G^{-1} = G_0^{-1} - \Sigma. \quad (37)$$

The same equation holds for holons

$$D_b^{-1} = d_b^{-1} - \Pi_b. \quad (38)$$

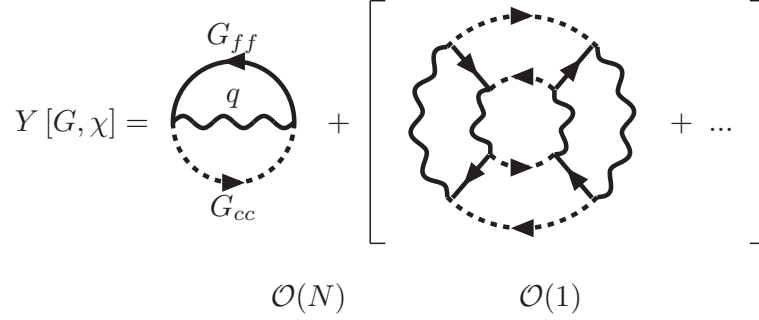


Figure 8. Leading skeleton diagrams participating to the LW functional Y_b for the Kondo Breakdown model with dependence on $1/N$. The fermionic propagators correspond to G_{ff} (straight line) and G_{cc} (dashed line) Green's functions of the zero order theory including the condensation part of the interaction. Both fermionic and bosonic propagators are fully dressed. The first diagram contains one fermionic loop carrying spin and channel quantum numbers and one pair of vertices, each of order $\mathcal{O}(1/\sqrt{N})$, so that it is of order $\mathcal{O}(N^2/N) = \mathcal{O}(N)$. The second diagram contains four loops and four pairs of vertices, so it is of order $\mathcal{O}(N^4/N^4) = \mathcal{O}(1)$.

One can manipulate gauge fluctuations in the same way as the above, where the gauge-coupling action, whose vertices are shown in Fig-9, is given by

$$\begin{aligned} \mathcal{S}_a^f &= \frac{1}{m_f} \sum_{k,q} \left| \mathbf{k} - \frac{\mathbf{q}}{2} \right| \left(a_q f_{\sigma k}^\dagger f_{\sigma k-q} + H.c. \right) + \frac{1}{2m_f} \sum_{k,q',q} a_{q'}^\dagger a_{q'+q} f_{\sigma k+q}^\dagger f_{\sigma k}, \\ \mathcal{S}_a^b &= \frac{1}{m_b} \sum_{q',q} \left| \mathbf{q}' - \frac{\mathbf{q}}{2} \right| \left(a_q b_{\sigma q'}^\dagger b_{\sigma q'-q} + H.c. \right) + \frac{1}{2m_b} \sum_{k,q',q} a_{q'}^\dagger a_{q'+q} b_{\sigma k+q}^\dagger b_{\sigma k}, \end{aligned} \quad (39)$$

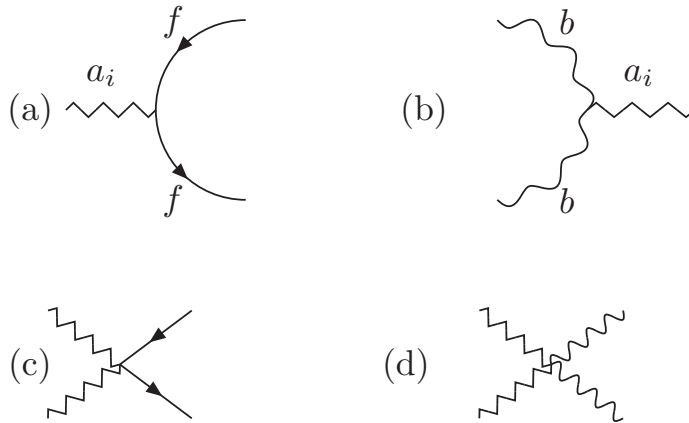


Figure 9. Vertices due to the interaction of the gauge fields with holons and spinons. Gauge propagator is represented by a zigzag line.

3.2.3. *Introduction of gauge fluctuations* Following exactly the same procedure for hybridization fluctuations, one finds the following additional terms in Eq.(35)

$$\begin{aligned}
F_a &= T \text{Tr} \left[\ln \left(-d_a^{-1} + \Pi_a \right) + \Pi_a D_a \right] \\
Y_a &= -\frac{NT^2}{2} \sum_{k,q \neq 0} F(q,k) G_{ff}(k) D_a(q) G_{ff}(k+q) \\
&\quad - \frac{T^2}{2} \sum_{q,q'} B(q,q') D_b(q) D_a(q') D_b(q+q'),
\end{aligned} \tag{40}$$

where

$$d_a^{-1}(\mathbf{q}, \Omega) = \frac{\Omega^2 + \mathbf{q}^2}{2g^2} + \frac{\mathcal{B}^2}{2m_b}, \quad D_a^{-1} \equiv d_a^{-1} - \Pi_a.$$

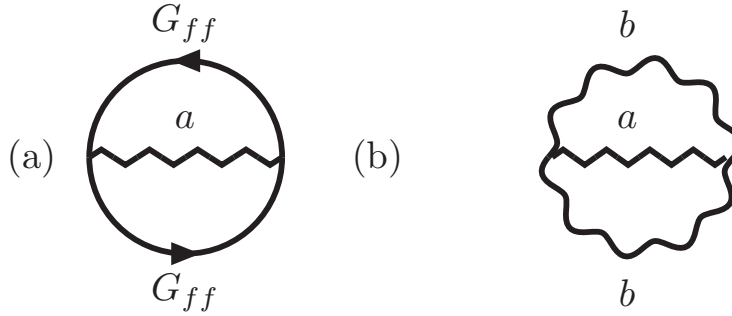


Figure 10. First order skeleton diagrams corresponding to Y_a . Fermionic and bosonic propagators are fully dressed.

$F(k, q)$ and $B(q, q')$ are the current-gauge bare vertices for spinons and holons given respectively by

$$\begin{aligned}
F(k, q) &\equiv \frac{1}{2} \sum_{i,j=1}^2 v_i^f \left(\delta_{ij} - \frac{q_i q_j}{q^2} \right) v_j^f, \quad v_i^f = \frac{k_i + q_i/2}{m_f}, \\
B(k, q) &\equiv \frac{1}{2} \sum_{i,j=1}^2 v_i^b \left(\delta_{ij} - \frac{q_i q_j}{q^2} \right) v_j^b, \quad v_i^b = \frac{k_i + q_i/2}{m_b},
\end{aligned}$$

Y_a corresponds to the contribution of the leading skeleton diagrams, due to interactions with the gauge field, constructed with the fully dressed propagators of the spinons, the holons and the gauge fields (see Fig-10).

3.3. Eliashberg equations

As for the HMM model, we can show that Eliashberg equations can be derived from the LW functional approach. Indeed, restricting ourselves to the leading $\mathcal{O}(N)$ terms of $Y = Y_b + Y_a$ shown in Fig-8 and Fig-10, one can derive, in the same manner as in the HMM case, the following expressions for the self-energies

$$\begin{aligned}
\Sigma_{cc}(k) &= 2V^2T \sum_q D_b(q)G_{ff}(k+q) \\
\Sigma_{ff}(k) &\equiv \Sigma_{ff}^a + \Sigma_{ff}^b \\
&= T \sum_q F(k,q)G_{ff}(k+q)D_a(q) + 2V^2T \sum_q G_{cc}(k-q)D_b(q) \\
\Pi_b(q) &\equiv \Pi_b^a + \Pi_b^c \\
&= T \sum_{q'} B(q,q')D_a(q')D_b(q+q') + NV^2T \sum_k G_{ff}(k+q)G_{cc}(k) \\
\Pi_a(q) &\equiv \Pi_a^f + \Pi_a^b \\
&= \frac{NT}{2} \sum_k F(k,q)G_{ff}(k)G_{ff}(k+q) + \frac{T}{2} \sum_{q'} B(q',q)D_b(q)D_b(q+q')
\end{aligned} \tag{41}$$

We see that the gauge field induces an additional part in the self-energies of the spinons and the holons, which we notice Σ_{ff}^a and Π_b^a respectively (See Fig-11).

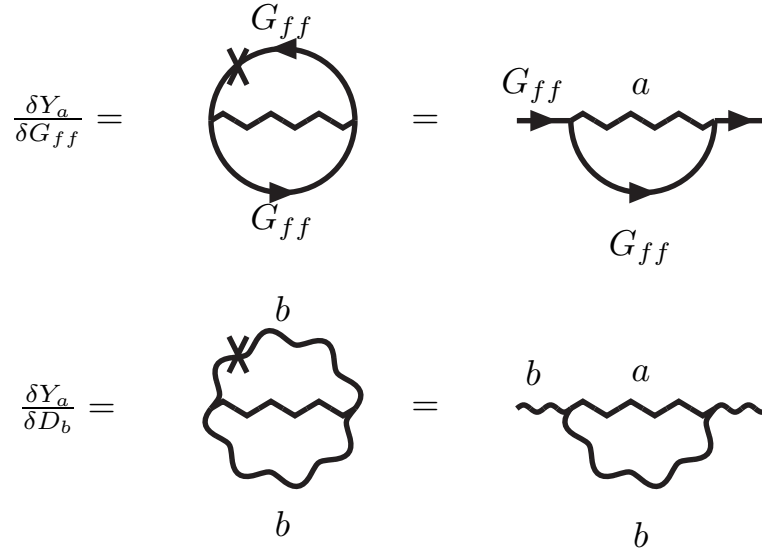


Figure 11. Illustrating functional derivative of the gauge part Y_a of LW functional with respect to Green's functions. The cross indicates the line that is cut by functional differentiation. Additional parts for the f-f channel and the holon self-energies are generated due to interactions with the gauge field.

Equations (41) are nothing but the Eliashberg equations for the KB model studied in [15]. It is found that this approximation becomes exact in the limit $N \rightarrow \infty$, provided we take into account the Fermi surface curvature[10].

3.4. Simplification of the Luttinger-Ward expression

We can notice that

$$\begin{aligned} Y_b &\equiv -2NV^2 \sum_k \sum_{q \neq 0} D_b(q) G_{cc}(k) G_{ff}(k+q) \\ &= NT \sum_k \Sigma_{cc}(k) G_{cc} + \Sigma_{ff}^b(k) G_{ff} \end{aligned} \quad (42)$$

$$= -T \sum_q \Pi_b^{fc}(q) D_b(q), \quad (43)$$

and that

$$\begin{aligned} Y_a &\equiv -\frac{NT^2}{2} \sum_{k, q \neq 0} F(q, k) G_{ff}(k) D_a(q) G_{ff}(k+q) \\ &\quad - \frac{T^2}{2} \sum_{q, q'} B(q, q') D_b(q) D_a(q') D_b(q+q') \\ &= NT \sum_k \Sigma_{ff}^a(k) G_{ff}(k) - \sum_q \Pi_b^a(q) D_b(q) \end{aligned} \quad (44)$$

$$= NT \sum_k \Sigma_{ff}^a(k) G_{ff}(k) - \sum_q \Pi_a^b(q) D_a(q) \quad (45)$$

Hence, we can simplify the expression of free energy for the KB model by introducing either equations (42-45) into the expression of the free energy. As an example, if we use Eq. (43) and (45) we get the following expression for free energy

$$F_{LW}^{eff} = F_F + F_b + F_a + (SN - \mathcal{B}^2)(\mu_b + ia_0) + u_b \frac{\mathcal{B}^4}{2},$$

with

$$\begin{aligned} F_F &= -T \text{Tr} \left[\ln(-G^{-1}) + \Sigma^b G \right] \\ F_b &= T \text{Tr} \left[\ln(-D_b^{-1}) + \Pi_b^a D_b \right] \\ F_a &= T \text{Tr} \left[\ln(-D_a^{-1}) \right] \end{aligned} \quad (46)$$

In this expression, the fermionic contribution reduces to a Fermi liquid form (see Appendix B.2)

$$F_{LW}^F \approx -\frac{\pi N \rho_+}{6} T^2 - \frac{\pi N \rho_-}{6} T^2,$$

where ρ_{\pm} is the density of states of the upper(lower) hybridized band. The singular part of the free energy is given solely by the bosonic sector : $F_s = F_a + F_b$.

We can make a further simplification considering that $\Pi_b^{fc} \gg \Pi_b^a$ +, in which case the holon part is given by

$$F_b = T \sum_q \ln \left(-d_b^{-1}(q) + \Pi_b^{fc}(q) \right).$$

+ In the non-condensed phase, $\mathcal{B} = 0$, the contribution of the gauge fields to the boson propagator has been shown [15] to be dominant only for $T \leq E^*$ as it is then the only source of damping for the bosons. In the condensed phase with $\mathcal{B} \neq 0$, Π_b^{fc} gets an additional term proportional to \mathcal{B}^2 . (See Eq. (31)) and is thus leading.

3.5. Thermodynamics

Performing the energy and momentum integrals in the Eliashberg equations [Eqs. (41)], we find Landau damping expressions for the holon and the gauge polarizations

$$\begin{aligned}\Pi_b^{fc}(q, i\Omega) &= \frac{\gamma_b}{2m_b} \frac{|\Omega|}{q}, \\ \Pi_a^f(q, i\Omega) + \Pi_a^b(q, i\Omega) &= \frac{\gamma_a}{2m_a} \frac{|\Omega|}{q},\end{aligned}\quad (47)$$

where

$$\gamma_b = \frac{2\pi}{v_F^f} \quad \frac{\gamma_a}{m_a} = \frac{N\pi}{m_f v_F^f} + \frac{\pi f_d}{m_b}$$

with $m_b = \frac{2}{NV^2\rho_c}$ and $f_d = \int \frac{d^{(d-1)}q^2}{(2\pi)^{(d-1)}d}$ with a UV cut-off [15].

The singular contribution for the free energy is

$$\begin{aligned}f_s(\mu_b, T) &= f_c(\mu_b, T) + T \sum_q \ln\left(q^2 + \gamma_b \frac{|\Omega|}{q} + \Delta_b(\mu_b, T)\right) \\ &+ T \sum_q \ln\left(q^2 + \gamma_a \frac{|\Omega|}{q} + \Delta_a(\mu_b, T)\right),\end{aligned}\quad (48)$$

where the condensation part $f_c(\mu_b, T)$, holon mass $\Delta_b(\mu_b, T)$, and gauge-boson mass $\Delta_a(\mu_b, T)$ are given by

$$\begin{aligned}f_c(\mu_b, T) &= -\mu_b \mathcal{B}^2 + \frac{u_b}{2} \mathcal{B}^4, \\ \Delta_b(\mu_b, T) &= -2m_b(\mu_b)[\mu_b - 2u_b \mathcal{B}^2(\mu_b, T)], \\ \Delta_a(\mu_b, T) &= \frac{m_a}{m_b(\mu_b)} \mathcal{B}^2(\mu_b, T),\end{aligned}\quad (49)$$

respectively. Note that the holon band mass depends on the effective chemical potential since it is given by the electron density of states. The coefficient in the gauge-boson mass is given by $\frac{m_a}{m_b(\mu_b > 0)} \approx \mathcal{O}(1) \left(\frac{V}{D}\right)^2$, approximately.

An important remark is that we can determine self-consistently the condensation value \mathcal{B} by the condition $\frac{\partial F_{LW}^{eff}}{\partial \mathcal{B}} = 0$ (See Appendix F). Beside the part obtained at the mean-field level, there are contributions due to hybridization and gauge fluctuation corrections. The Eliashberg framework allows then to refine the value of the condensation \mathcal{B} .

An explicit analytic expression for the singular part of the free energy is obtained after integration on frequencies and momenta in Eq.(48). The details of this evaluation for $d = 3, z = 3$ and its results are given in Appendix D.

3.6. Scaling of the free energy near the Kondo breakdown quantum critical point

Once we have the analytic expression for the singular part of the free energy, after integration of frequencies and momenta in Eq.(48), we can deduce its scaling expressions.

As shown previously, this part of the free energy results from collective boson excitations associated with hybridization and gauge fluctuations. For each of these bosonic excitations, we associate a length scale for such boson excitations, and the scaling form of the free energy near the Kondo Breakdown QCP reads

$$f_s(\xi_b^{-2}, \lambda_a^{-2}, T) = b_b^{-(d+z_b)} f_b(\xi_b^{-2} b_b^{1/\nu_b}, T b_b^{z_b}) + b_a^{-(d+z_a)} f_a(\lambda_a^{-2} b_a^{1/\nu_a}, T b_a^{z_a}). \quad (50)$$

$f_{b(a)}(x, y)$ is an analytic regular function for hybridization (gauge) fluctuations and d is the space dimension. $\xi_b = \Delta_b^{-1/2}$ is the correlation length for holons, and $\lambda_a = \Delta_a^{-1/2}$ is the one for gauge bosons. In particular, λ_a may be considered as the penetration depth in the superconductor. b_b and b_a are scaling parameters for hybridization and gauge fluctuations, respectively*. $\nu_{b(a)}$ is the correlation-length exponent of holons (gauge bosons), and $z_{b(a)}$ is the dynamical exponent of holons (gauge bosons). Here we have $z_b = z_a$ as shown in Eq. (47). Furthermore, $\nu_b = \nu_a = 1/2$ as there are no quantum corrections to the usual Ornstein-Zernicke form of a static boson propagator within the Eliashberg treatment. These values for $\nu_{a,b}$ coincide with the mean-field value of the correlation length critical exponent in Hertz theory above its upper critical dimension.

Although two kinds of length scales are introduced, both scales diverge at the same parameter point, $V = V_c$ because they are related with each other via Anderson-Higgs mechanism. In addition, we note that this expression is applicable near the Kondo breakdown QCP, approaching from the heavy-fermion side because we have considered properly and in a self-consistent way the effect of a finite condensation.

Inserting $b_b = \xi_b^{2\nu}$ and $b_a = \lambda_a^{2\nu}$ into the above scaling expression, we find

$$f_s(\xi_b^{-2}, \lambda_a^{-2}, T) = \xi_b^{-2\nu(d+z)} f_b(1, T \xi_b^{2\nu z}) + \lambda_a^{-2\nu(d+z)} f_a(1, T \lambda_a^{2\nu z}). \quad (51)$$

This is our main result, derived from the microscopic model based on the LW functional approach in the Eliashberg framework. Now, one can understand thermodynamics near the Kondo breakdown QCP based on this scaling free energy.

4. Discussion and summary

In this study we derived the scaling of free energy from a microscopic model for two models of quantum criticality : the standard theoretical framework called the Hertz-Moriya-Millis (HMM) theory and the strong coupling approach corresponding to the gauge theory. Fluctuation corrections are taken into account systematically in the Luttinger-Ward functional approach. The Eliashberg framework allows to use the proper level of approximation to get, self-consistently, the correct scaling for thermodynamics near the quantum critical point (QCP). We have shown that the singular part of the free energy for both models is due to the collective bosonic excitations, whereas the fermionic excitations give a Fermi Liquid contribution.

* These scaling factors are in fact the same but may be associated with different dynamical exponents for different parts of the bosonic sector. Thus, we introduce subscripts for holons and gauge bosons to keep in mind this fact.

For the HMM theory, there exists one length scale associated with the corresponding symmetry breaking, here spin-density-wave (SDW) instability. This fact allows us to construct the scaling free energy as a function of the spin-spin correlation length and temperature for the SDW quantum transition. We derived the correct scaling expression using the Luttinger-Ward functional approach in the Eliashberg framework.

For the gauge theory, there are additional collective excitations. These have nothing to do with the phase transition directly although they are affected by it. Such collective modes turn out to be gauge fluctuations corresponding to collective spin fluctuations in our context. An additional length scale, associated with gauge fluctuations, can appear. Indeed, considering that the Kondo breakdown transition is driven by condensation of holons, corresponding to the formation of an effective hybridization, the structure of the theory gives rise to massive gauge fluctuations via the Anderson-Higgs mechanism. This is the physical reason why the second length scale appears in the gauge theory.

Because the two kinds of length scales, correlation length of hybridization fluctuations and penetration depth of gauge fluctuations, are deeply related via the Anderson-Higgs mechanism, they diverge at the Kondo breakdown QCP simultaneously. However, the presence of the additional length scale leads to a different scaling expression for the thermodynamic potential, compared with the HMM theory. We derived such a scaling expression using the Luttinger-Ward functional approach in the Eliashberg framework. In the Eliashberg approximation, we showed that the scaling expression of the free energy has two contributions corresponding to each length scale, where each part contains only one length scale.

In this paper we ignored vertex corrections, sometimes justified but not always [10]. Our path integral derivation of the Luttinger-Ward functional gives a chance to extend the Eliashberg framework, allowing vertex corrections. This can be achieved by going to higher orders of the cumulant expansion. In particular, if we do the same job up to the fourth order, we expect that vertex corrections will appear, satisfying the Bethe-Salpeter equation for vertices [23]. It is an important future direction to see how introduction of vertex corrections changes the scaling expression of the Eliashberg approximation.

This work is supported by the French National Grant ANR26ECCEZZZ.

Appendix A. Derivation of the Luttinger-Ward functional up to second order in the interaction

The LW functional can be derived thoroughly using a cumulant expansion to the second order in the interaction term. Indeed, this term induces the following corrections to the bare action

$$\begin{aligned}
\delta\mathcal{S}_0 \approx & -g^2 T^4 \sum_{k,k'} \sum_{q,q'} \left[\psi_{\alpha k}^\dagger \langle \psi_{\beta k} \psi_{\alpha'k'+q}^\dagger \tau_{\alpha\beta}^n S_{-q}^m \tau_{\alpha'\beta'}^m S_{-q'}^m \rangle_c \psi_{\beta'k'} \right. \\
& + \langle \psi_{\beta k} \psi_{\alpha'k'+q}^\dagger \tau_{\alpha\beta}^n S_{-q}^m \tau_{\alpha'\beta'}^m S_{-q'}^m \rangle_c \langle \psi_{\alpha k+q}^\dagger \psi_{\beta'k'} \rangle_c + \psi_{\alpha k}^\dagger \langle \psi_{\alpha'k'+q} \psi_{\beta'k'}^\dagger \tau_{\alpha\beta}^n S_{-q}^m \tau_{\alpha'\beta'}^m S_{-q'}^m \rangle_c \psi_{\beta k} \\
& + \langle \psi_{\alpha'k'+q} \psi_{\beta'k'}^\dagger \tau_{\alpha\beta}^n S_{-q}^m \tau_{\alpha'\beta'}^m S_{-q'}^m \rangle_c \langle \psi_{\alpha k+q}^\dagger \psi_{\beta k} \rangle_c \left. \right] \\
& - \frac{g^2}{2} T^4 \sum_{k,k'} \sum_{q,q'} \left[S_{-q}^n \langle \psi_{\alpha k+q}^\dagger \tau_{\alpha\beta}^n \psi_{\beta k} \psi_{\alpha'k'+q}^\dagger \tau_{\alpha'\beta'}^m \psi_{\beta'k'} \rangle_c S_{-q'}^m \right. \\
& + \langle \psi_{\alpha k+q}^\dagger \tau_{\alpha\beta}^n \psi_{\beta k} \psi_{\alpha'k'+q}^\dagger \tau_{\alpha'\beta'}^m \psi_{\beta'k'} \rangle_c \langle S_{-q}^n S_{-q'}^m \rangle_c \left. \right] \\
& - \frac{g^2}{2} T^4 \sum_{k,k'} \sum_{q,q'} \left[\langle \psi_{\alpha k+q}^\dagger \psi_{\beta'k'} \rangle_c \tau_{\alpha\beta}^n \tau_{\alpha'\beta'}^m \langle S_{-q}^n S_{-q'}^m \rangle_c \langle \psi_{\beta k} \psi_{\alpha'k'+q}^\dagger \rangle_c \right. \\
& + \langle \psi_{\alpha k+q}^\dagger \psi_{\beta k} \rangle_c \tau_{\alpha\beta}^n \tau_{\alpha'\beta'}^m \langle S_{-q}^n S_{-q'}^m \rangle_c \langle \psi_{\alpha'k'+q}^\dagger \psi_{\beta'k'} \rangle_c \left. \right], \tag{A.1}
\end{aligned}$$

The fermionic and bosonic propagators are introduced as

$$G(k)\delta_{kk'}\delta_{\sigma\sigma'} \equiv -\langle \psi_{\sigma k} \psi_{\sigma'k'}^\dagger \rangle_c, \quad \chi(q)\delta_{qq'} \equiv \langle S_q^n S_{-q'}^m \rangle_c$$

while the corresponding self-energies are

$$\begin{aligned}
\Sigma(k)\delta_{kk'}\delta_{qq'}\delta_{\beta\alpha'} & \equiv -g^2 \langle \psi_{\beta k} \psi_{\alpha'k'+q}^\dagger \tau_{\alpha\beta}^n S_{-q}^m \tau_{\alpha'\beta'}^m S_{-q'}^m \rangle_c \\
& - g^2 \langle \psi_{\alpha'k'+q} \psi_{\beta'k'}^\dagger \tau_{\alpha\beta}^n S_{-q}^m \tau_{\alpha'\beta'}^m S_{-q'}^m \rangle_c, \\
\Pi(q)\delta_{qq'} & \equiv -g^2 \langle \psi_{\alpha k+q}^\dagger \tau_{\alpha\beta}^n \psi_{\beta k} \psi_{\alpha'k'+q}^\dagger \tau_{\alpha'\beta'}^m \psi_{\beta'k'} \rangle_c.
\end{aligned}$$

The two last sums in (A.1) corresponds to the two diagrams shown in Fig-A1 where the fermionic and bosonic propagators are bare.

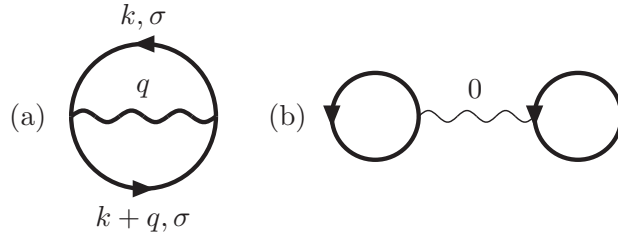


Figure A1. The one loop closed diagrams for free energy in the SF model. The fermionic and bosonic propagators are bare

The prescription to get the LW functional at this order is to dress these propagators[4] in the corresponding skeleton diagram, resulting in the following

expression for the LW functional

$$Y = N \frac{3g^2}{2} T^2 \sum_{k,q} G(k) \chi(q) G(k+q) + N^2 \frac{3g^2}{2} T^2 \chi(0) \sum_k G(k) \sum_{k'} G(k'). \quad (\text{A.2})$$

In Fig-A1, the diagram (b) will generate a static and uniform part in the self-energy and can thus be considered as a renormalization of the electron chemical potential.

Appendix B. Fermionic contribution to free energy

Appendix B.1. Spin-fermion model

The momentum dependence of the electron self-energy is shown to be regular [10], we then replace the momentum with the Fermi momentum k_F : $\Sigma(i\omega) \equiv \Sigma(\mathbf{k}_F, i\omega)$. Then, the electron contribution to the free energy of the SF model is given by

$$\begin{aligned} F_{el} &\equiv -NT \sum_{i\omega, k} \left[\ln \left\{ -G_0^{-1}(k, i\omega) + \Sigma(i\omega) \right\} + \Sigma(i\omega) G(k, i\omega) \right] \\ &= -NT \sum_{i\omega, k} \left[\int_0^1 du \partial_u \ln \left\{ -G_0^{-1}(k, i\omega) + u \Sigma(i\omega) \right\} \right. \\ &\quad \left. + \frac{\Sigma(i\omega)}{G_0^{-1}(k, i\omega) - \Sigma(i\omega)} \right] - NT \sum_{i\omega, k} \ln \left\{ -G_0^{-1}(k, i\omega) \right\} \end{aligned} \quad (\text{B.1})$$

Here, the last term corresponds to the free fermion part giving raise to the Fermi liquid form of the free energy for electrons

$$-NT \sum_{i\omega, k} \ln \left\{ -G_0^{-1}(k, i\omega) \right\} = -N \frac{\pi \rho_F}{6} T^2, \quad (\text{B.2})$$

where ρ_F is the density of states at the Fermi level. The first two terms of (B.1) are shown to be vanishingly small in the low energy limit. Indeed, we have

$$\begin{aligned} \delta F_{el} &\equiv -NT \sum_{i\omega, k} \left[\int_0^1 du \partial_u \ln \left\{ -G_0^{-1}(k, i\omega) + u \Sigma(i\omega) \right\} + \frac{\Sigma(i\omega)}{G_0^{-1}(k, i\omega) - \Sigma(i\omega)} \right] \\ &= -NT \sum_{i\omega, k} \int_0^1 du \left[-\frac{\Sigma(i\omega)}{G_0^{-1}(k, i\omega) - u \Sigma(i\omega)} + \frac{\Sigma(i\omega)}{G_0^{-1}(k, i\omega) - \Sigma(i\omega)} \right] \\ &= -NT \sum_{i\omega, k} \frac{\Sigma(i\omega)^2}{G_0^{-1}(k, i\omega) - \Sigma(i\omega)} \int_0^1 du \frac{(1-u)}{G_0^{-1} - u \Sigma}. \end{aligned} \quad (\text{B.3})$$

Now, we can switch from the integration over momentum to that over energy as follows

$$\sum_k \dots \rightarrow \rho_F \int_{-\Lambda}^{\Lambda} d\epsilon \dots$$

where Λ is an energy cut-off.

Integrating over ϵ , we find that

$$\delta F_{el} = -NT \rho_F \int_0^1 du \sum_{i\omega} \Sigma(i\omega) \left[\ln \left(\frac{i\omega - \Sigma(i\omega) - \Lambda}{i\omega - \Sigma(i\omega) + \Lambda} \right) - \ln \left(\frac{i\omega - u \Sigma(i\omega) - \Lambda}{i\omega - u \Sigma(i\omega) + \Lambda} \right) \right]$$

For $|u\Sigma(i\omega)| \ll \Lambda$, the two last terms cancels and δF_{el} vanishes. The electronic part of the free energy (12) of the SF model reduces then to the Fermi liquid contribution

$$F_{el} = -N \frac{\pi \rho_F}{6} T^2. \quad (\text{B.4})$$

Appendix B.2. Kondo breakdown theory

The fermionic sector in the KB model factorizes into an upper (+) and a lower (-) band whose dispersions are given by

$$E_{\mathbf{k}\pm} = \frac{1}{2} \left[\epsilon_{\mathbf{k}} + \epsilon_{\mathbf{k}}^0 \pm \sqrt{(\epsilon_{\mathbf{k}} - \epsilon_{\mathbf{k}}^0)^2 + 4V^2 \mathcal{B}^2} \right]$$

The free energy for each band has a similar expression to Eq. (B.4) and reduces to a Fermi liquid form

$$F_{\pm} = -\frac{\pi N \rho_{\pm}}{6} T^2,$$

where ρ_{\pm} is the density of states of the upper (lower) band at the Fermi level given by

$$\rho_{\pm} = \rho_0 \left(\frac{\partial E_{\mathbf{k}\pm}}{\partial \epsilon_{\mathbf{k}}} \right)_{|E_{\pm}=0}^{-1}$$

Appendix C. Momentum and frequency integral for the free energy of the Spin-fermion model

Introducing $f(x) = \tan^{-1} x$, we have the following limits

$$f(x \ll 1) \approx x, \quad f(x \gg 1) \approx \frac{\pi}{2}. \quad (\text{C.1})$$

Then, the free energy expression of Eq. (17) can be cast according to

$$f_s(\xi, T) \approx -\frac{1}{2\pi^3} \int_0^{\infty} d\nu \coth\left(\frac{\nu}{2T}\right) \left[\frac{\nu}{\Omega_s} \int_{q_r}^{\infty} d\tilde{q} \frac{\tilde{q}^2}{\xi^{-2} + \tilde{q}^2} + \frac{\pi}{2} \int_0^{q_r} d\tilde{q} \tilde{q}^2 \right], \quad (\text{C.2})$$

where $q_r = \sqrt{\frac{\nu}{\Omega_s} - \xi^{-2}}$. Then

$$\begin{aligned} f_s(\xi, T) &= -\frac{1}{2\pi^3} \int_0^{\infty} d\nu \coth\left(\frac{\nu}{2T}\right) \left[\frac{\nu}{\Omega_s} \left\{ \Lambda_q - \sqrt{\frac{\nu}{\Omega_s} - \xi^{-2}} \right. \right. \\ &\quad \left. \left. - \xi^{-1} \left(\frac{\pi}{2} - \tan^{-1} \sqrt{\frac{\xi^2 \nu}{\Omega_s} - 1} \right) \right\} + \frac{\pi}{6} \left(\frac{\nu}{\Omega_s} - \xi^{-2} \right)^{3/2} \right] \\ &\approx -\frac{1}{2\pi^3} \frac{(2T)^2}{\Omega_s} \Lambda_q + \xi^{-5} f_r(T\xi^2), \end{aligned} \quad (\text{C.3})$$

where Λ_q is a momentum cutoff and

$$\begin{aligned} f_r(T\xi^2) &= \frac{1}{2\pi^3} \left[\frac{[2T\xi^2]^2}{\Omega_s} \left\{ \sqrt{\frac{2T\xi^2}{\Omega_s} - 1} + \left(\frac{\pi}{2} - \tan^{-1} \sqrt{\frac{2T\xi^2}{\Omega_s} - 1} \right) \right\} \right. \\ &\quad \left. - \frac{\pi}{6} [2T\xi^2] + \left(\frac{[2T\xi^2]}{\Omega_s} - 1 \right)^{\frac{3}{2}} \right]. \end{aligned}$$

We see that the singular part of the free energy follows the scaling relation shown in Eqs. (18) and (19).

Appendix D. Momentum and frequency integral for the free energy in the Kondo breakdown scenario

Let's consider the spectral representation of Eq. (48)

$$f_s(\mu_r, T) = f_c(\mu_r, T) - \frac{1}{2\pi^3} \int_0^\infty d\nu \coth\left(\frac{\nu}{2T}\right) \int_0^\infty dq q^2 \left\{ \tan^{-1}\left(\gamma_b \frac{\nu}{q[q^2 + \Delta_b]}\right) + \tan^{-1}\left(\gamma_a \frac{\nu}{q[q^2 + \Delta_a]}\right) \right\}. \quad (\text{D.1})$$

Considering the approximation for $\tan^{-1} x$, the holon part is cast, as previously, into two parts in the momentum integral

$$\begin{aligned} f_b(\mu_b, T) &= -\frac{1}{2\pi^3} \int_0^\infty d\nu \coth\left(\frac{\nu}{2T}\right) \int_0^\infty dq q^2 \tan^{-1}\left(\gamma_b \frac{\nu}{q[q^2 + \Delta_b]}\right) \\ &\approx -\frac{1}{2\pi^3} \int_0^\infty d\nu \coth\left(\frac{\nu}{2T}\right) \int_{q_r}^\infty dq q^2 \frac{\gamma_b \nu}{q[q^2 + \Delta_b]} \\ &\quad - \frac{1}{2\pi^3} \int_0^\infty d\nu \coth\left(\frac{\nu}{2T}\right) \int_0^{q_r} dq q^2 \frac{\pi}{2}, \end{aligned}$$

where q_r is a characteristic momentum determined by the equation

$$\frac{\gamma_b \nu}{q_r[q_r^2 + \Delta_b]} = 1 \rightarrow q_r^3 + \Delta_b q_r - \gamma_b \nu = 0.$$

The solution of the latter is given by

$$q_r = -\frac{(2/3)^{1/3} \Delta_b}{\left(9\gamma_b \nu + \sqrt{12\Delta_b^3 + 81(\gamma_b \nu)^2}\right)^{1/3}} + \frac{\left(9\gamma_b \nu + \sqrt{12\Delta_b^3 + 81(\gamma_b \nu)^2}\right)^{1/3}}{2^{1/3} 3^{2/3}}, \quad (\text{D.2})$$

which is definitely positive.

Then

$$\begin{aligned} f_b(\mu_b, T) &= -\frac{1}{4\pi^3} \int_0^\infty d\nu \coth\left(\frac{\nu}{2T}\right) \int_{q_r}^{\Lambda_q^2} dx \frac{\gamma_b \nu}{x + \Delta_b} - \frac{1}{12\pi^2} \int_0^\infty d\nu \coth\left(\frac{\nu}{2T}\right) q_r^3 \\ &\approx -\frac{1}{4\pi^3} \int_0^\infty d\nu \coth\left(\frac{\nu}{2T}\right) \gamma_b \nu \ln\left(\frac{\Lambda_q^2 q_r}{\gamma_b \nu}\right) - \frac{1}{12\pi^2} \int_0^\infty d\nu \coth\left(\frac{\nu}{2T}\right) (-\Delta_b q_r + \gamma_b \nu), \end{aligned} \quad (\text{D.3})$$

where the momentum cutoff Λ_q is taken much larger than the holon mass, i.e., $\Lambda_q^2 \gg \Delta_b$.

The frequency integral can be performed approximately, given by

$$\begin{aligned} f_b(\mu_r, T) &= -\frac{1}{4\pi^3} \int_0^\infty d\nu \coth\left(\frac{\nu}{2T}\right) \gamma_b \nu \ln\left(\frac{\Lambda_q^2 q_r}{\gamma_b \nu}\right) - \frac{1}{12\pi^2} \int_0^\infty d\nu \coth\left(\frac{\nu}{2T}\right) (-\Delta_b q_r + \gamma_b \nu) \\ &\approx -\frac{1}{4\pi^3} \left\{ \int_0^{2T} d\nu \frac{2T}{\nu} + \int_{2T}^{\Lambda_\nu} d\nu \right\} \gamma_b \nu \ln\left(\frac{\Lambda_q^2 q_r [\Delta_b, \nu]}{\gamma_b \nu}\right) \\ &\quad - \frac{1}{12\pi^2} \left\{ \int_0^{2T} d\nu \frac{2T}{\nu} + \int_{2T}^{\Lambda_\nu} d\nu \right\} (-\Delta_b q_r + \gamma_b \nu) \\ &\approx -\frac{1}{4\pi^3} \int_0^{2T} d\nu \frac{2T}{\nu} \gamma_b \nu \ln\left(\frac{\Lambda_q^2 q_r [\Delta_b, \nu]}{\gamma_b \nu}\right) - \frac{1}{12\pi^2} \int_0^{2T} d\nu \frac{2T}{\nu} (-\Delta_b q_r + \gamma_b \nu) \\ &\approx -\frac{1}{4\pi^3 \gamma_b} (2\gamma_b T)^2 \ln\left(\frac{\Lambda_q^2 q_r [\Delta_b, 2T]}{2\gamma_b T}\right) - \frac{1}{12\pi^2 \gamma_b} (2\gamma_b T) (-\Delta_b q_r [\Delta_b, 2T] + 2\gamma_b T), \end{aligned}$$

where

$$q_r[\Delta_b, 2T] = - \frac{(2/3)^{1/3} \Delta_b}{\left(9[2\gamma_b T] + \sqrt{12\Delta_b^3 + 81(2\gamma_b T)^2}\right)^{1/3}} + \frac{\left(9[2\gamma_b T] + \sqrt{12\Delta_b^3 + 81(2\gamma_b T)^2}\right)^{1/3}}{2^{1/3} 3^{2/3}}. \quad (\text{D.4})$$

For the gauge-fluctuation part, exactly the same procedure is performed, and the result holds provided that the subscript b is replaced with a .

Appendix E. Introduction of dangerously irrelevant variables

In this appendix, we show how the presence of a dangerously irrelevant variable can affect the naive scaling relations obtained in (18) and (51)

We recall that Millis [1] showed in this case, using perturbative RG, that the control parameter $\delta = \xi_0^{-2}$ is renormalized according to

$$\delta_r = \delta + u \frac{C}{z + d - 2}, \quad (\text{E.1})$$

where C is a constant, and the correlation length ξ gets a temperature dependence

$$\xi^{-2} = \delta_r + g(d, z) u T^{\frac{d+z-2}{z}}, \quad (\text{E.2})$$

where g is a function depending on the dimension d and the dynamical exponent z .

Accordingly, the naive scaling shown in Eq.(18) is invalidated and the effect of the dangerously irrelevant parameter u must be incorporated into a generalized scaling form

$$f(\xi^{-2}, T, u) = b^{-(d+z)} f(\xi^{-2} b^{1/\nu}, T b^z, u b^{d+z-4}). \quad (\text{E.3})$$

Let's consider then a ϕ^4 term with a constant coefficient u in the SF model (4), as in the Hertz-Millis theory, within our method. The corresponding vertex is shown in Fig.- E1-(a) below. At the first loop level, this quartic term generates the diagrams shown in Fig.- E1-(b) and (c), where the bosonic propagators are full. These are of order $\mathcal{O}(1)$ and are thus sub-leading with respect to the diagram of order $\mathcal{O}(N)$ first considered in the LW functional shown in Fig.- 2.

If these are included in the LW functional, the bosonic self-energy, generated by variation of the free energy with respect to the bosonic Green's function as explained in section 2.4, gets a constant contribution from the diagram (a). This is a renormalization of the bosonic chemical potential as in Eq.(E.1). The diagram (b) is easily shown to give corrections to scaling to the correlation length ξ as

$$\xi^{-2}(T) - \xi^{-2}(0) \propto T^{\frac{d+z-2}{z}},$$

consistent with (E.2)

We see that our method allows to account self-consistently for the effect of the parameter u . Rigorously, this should be considered in the expression of the free energy.

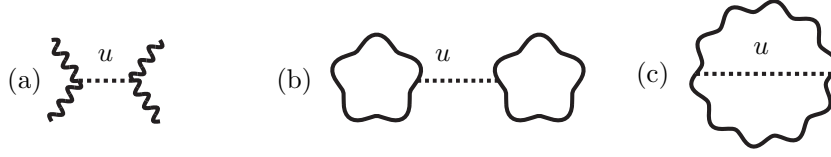


Figure E1. (a) a ϕ^4 vertex with a constant coefficient u , (b) and (c) are the first loop diagrams generated by the vertex (a) where the bosonic lines are fully dressed.

Our purpose in the main text is only to show how an analytic expression for free energy can be obtained in a self-consistent way.

Similar considerations should hold for the Kondo breakdown scenario as well. However, in practice, the naive scaling for the free energy can still be used to fit experimental data. This has been done in one of our previous papers [12] in the case of the Kondo Breakdown scenario to account for the anomalous exponent of the Grüneisen ratio of the compound $\text{YbRh}_2(\text{S}_{0.95}\text{Ge}_{0.05})_2$. The naive scaling for free energy gives a rather good agreement with the experiment in this case.

Appendix F. Self-consistent equation for \mathcal{B}

Minimizing the free energy Eq.46 with respect to \mathcal{B} , we get the following expression

$$0 = H_{MF}(\mathcal{B}) + T \sum_{i\Omega} \int \frac{d^d q}{(2\pi)^d} \frac{8m_b u_b \mathcal{B}}{q^2 + \gamma_b \frac{|\Omega|}{q} - 2m_b [\mu_b - 2u_b \mathcal{B}^2]} + T \sum_{i\Omega} \int \frac{d^d q}{(2\pi)^d} \frac{\frac{2m_a}{m_b} \mathcal{B}}{q^2 + \gamma_a \frac{|\Omega|}{q} + \frac{m_a}{m_b} \mathcal{B}^2}, \quad (\text{F.1})$$

where $H_{MF}(\mathcal{B}) = 0$ determines the mean-field value of the condensation \mathcal{B} . Fluctuations of the holon and the gauge fields result in additional terms in the self-consistent equation for \mathcal{B} .

The holon part is evaluated as follows

$$\begin{aligned} T \sum_{i\Omega} \int \frac{d^3 q}{(2\pi)^3} \frac{1}{q^2 + \gamma_b \frac{|\Omega|}{q} + \Delta_b} &= \int \frac{d^3 q}{(2\pi)^3} \int_{-\infty}^{\infty} d\nu \left(-\frac{1}{\pi}\right) \frac{\gamma_b \nu / q}{(q^2 + \Delta_b)^2 + (\gamma_b \nu)^2 / q^2} T \sum_{i\Omega} \frac{1}{i\Omega - \nu} \\ &= \frac{1}{2\pi^3} \int_0^{\infty} d\nu \coth\left(\frac{\nu}{2T}\right) \int_0^{\infty} dq \frac{\gamma_b \nu q^3}{q^2 (q^2 + \Delta_b)^2 + (\gamma_b \nu)^2} \\ &= \frac{1}{4\pi^3} \int_0^{\infty} d\nu \coth\left(\frac{\nu}{2T}\right) \int_0^{\infty} dx \frac{\gamma_b \nu x}{x(x + \Delta_b)^2 + (\gamma_b \nu)^2} \\ &\approx \frac{1}{4\pi^3} \int_0^{\infty} d\nu \coth\left(\frac{\nu}{2T}\right) \int_{\text{Max}[\Delta_b, (\gamma_b \nu)^{2/3}]}^{\infty} dx \frac{\gamma_b \nu x}{x^3} \\ &= \frac{1}{4\pi^3} \int_0^{\infty} d\nu \coth\left(\frac{\nu}{2T}\right) \frac{\gamma_b \nu}{\text{Max}[\Delta_b, (\gamma_b \nu)^{2/3}]} \\ &\approx \frac{1}{4\pi^3 \gamma_b} \frac{(2\gamma_b T)^2}{\text{Max}[\Delta_b, (2\gamma_b T)^{2/3}]}, \end{aligned} \quad (\text{F.2})$$

where the Max function is defined as $\text{Max}[A, B] = A$ when $A \geq B$.

The gauge part is evaluated in the same way and the analytic expression for the self-consistent equation of \mathcal{B} writes

$$0 = H_{MF}(\mathcal{B}) + \frac{m_b u_b}{\pi^3 \gamma_b} \frac{\mathcal{B}(2\gamma_b T)^2}{\text{Max}[-2m_b(\mu_b - 2u_b \mathcal{B}^2), (2\gamma_b T)^{2/3}]} + \frac{m_a/m_b}{4\pi^3 \gamma_a} \frac{\mathcal{B}(2\gamma_a T)^2}{\text{Max}[\frac{m_a}{m_b} \mathcal{B}^2, (2\gamma_a T)^{2/3}]} \quad (\text{F.3})$$

- [1] T. Moriya and J. Kawabata, J. Phys. Soc. Jpn. **34**, 639 (1973); T. Moriya and J. Kawabata, J. Phys. Soc. Jpn. **35**, 669 (1973); J. A. Hertz, Phys. Rev. B **14**, 1165 (1976); A. J. Millis, Phys. Rev. B **48**, 7183 (1993).
- [2] P. A. Lee, N. Nagaosa, and X.-G. Wen, Rev. Mod. Phys. **78**, 17 (2006), and references therein.
- [3] P. Coleman, C. Pépin, Q. Si, R. Ramazashvili, Journal of Physics: Condensed Matter **13**, 723 (2001).
- [4] J. M. Luttinger and J. C. Ward, Phys. Rev. **118**, 1417 (1960).
- [5] G. Baym and L. P. Kadanoff, Phys. Rev. **124**, 287 (1961).
- [6] P. Coleman, I. Paul, and J. Rech, Phys. Rev. B **72**, 094430 (2005).
- [7] M. Potthoff, Condens. Mat. Phys. **9**, 557 (2006).
- [8] R. Chitra and G. Kotliar, Phys. Rev. B **63**, 115110 (2001).
- [9] A. V. Chubukov, D. L. Maslov, S. Gangadharaiah, and L. I. Glazman, Phys. Rev. B **71**, 205112 (2005).
- [10] J. Rech, C. Pépin, and A. V. Chubukov, Phys. Rev. B **74**, 195126 (2006).
- [11] A. V. Chubukov, Phys. Rev. B **72**, 085113 (2005).
- [12] K.-S. Kim, A. Benlagra, and C. Pépin, Phys. Rev. Lett. **101**, 246403 (2008).
- [13] T. Senthil, M. Vojta, and S. Sachdev, Phys. Rev. B **69**, 035111 (2004).
- [14] I. Paul, C. Pépin, and M. R. Norman, Phys. Rev. Lett. **98**, 026402 (2007); Phys. Rev. B **78**, 035109 (2008).
- [15] C. Pépin, Phys. Rev. Lett. **98**, 206401 (2007); Phys. Rev. B **77**, 245129 (2008).
- [16] J. Custers, P. Gegenwart, H. Wilhelm, K. Neumaier, Y. Tokiwa, O. Trovarelli, C. Geibel, F. Steglich, C. Pepin, and P. Coleman, Nature **424**, 524 (2003).
- [17] A. Schroder, G. Aeppli, R. Coldea, M. Adams, O. Stockert, H.v. Lohneysen, E. Bucher, R. Ramazashvili, and P. Coleman, Nature **407**, 351 (2000).
- [18] H. Shishido, R. Settai, H. Harima, and Y. Onuki, J. Phys. Soc. Jpn. **74**, 1103 (2005).
- [19] S. Paschen, T. Luhmann, S. Wirth, P. Gegenwart, O. Trovarelli, C. Geibel, F. Steglich, P. Coleman, and Q. Si, Nature **432**, 881 (2004).
- [20] R. Kuchler, N. Oeschler, P. Gegenwart, T. Cichorek, K. Neumaier, O. Tegus, C. Geibel, J. A. Mydosh, F. Steglich, L. Zhu, and Q. Si, Phys. Rev. Lett. **91**, 066405 (2003).
- [21] Ar. Abanov, A. V. Chubukov, J. Schmalian, Adv. Phys. **52**119 (2003)
- [22] A. V. Chubukov, D. Pines, J. Schmalian, "Physics of conventional and unconventional Superconductors", Vol. I, ed. K. H. Bennemann and J. B. Ketterson (Springer, Berlin, 2004), p.1349
- [23] V. Janis, arXiv:cond-mat/9806118.
- [24] L. De Leo, M. Civelli, and G. Kotliar, Phys. Rev. Lett. **101**, 256404 (2008)
- [25] K.-S. Kim and C. Pépin, Phys. Rev. Lett. **102** 156404 (2009)